Sensitivities on nonspinning and spinning primordial black hole dark matter with global 21-cm troughs

Akash Kumar Saha[*] and Ranjan Laha[†]

Centre for High Energy Physics, Indian Institute of Science, C. V. Raman Avenue, Bengaluru 560012, India

(Received 29 December 2021; accepted 11 April 2022; published 24 May 2022)

Detection of the global 21 cm signal arising from neutral hydrogen can revolutionize our understanding of the standard evolution of the Universe after recombination. In addition, it can also be an excellent probe of dark matter (DM). Among all the DM candidates, primordial black holes (PBHs) are one of the most well motivated. Hawking emission from low-mass PBHs can have a substantial effect on the thermal and ionization history of the early Universe, and that in turn can have an imprint on the global 21 cm signal. Recently EDGES has claimed a global 21 cm signal, though SARAS 3 has rejected that claim. In this work, we investigate the sensitivities on nonspinning and spinning PBHs arising from an EDGES-like measurement of the global 21 cm signal, and find that the sensitivities will be competitive with those arising from other astrophysical observables. We show that the sensitivities can be significantly strengthened depending on various uncertain astrophysical parameters. Besides, we also derive projections on the PBH density from the absorption trough expected during the Dark Ages. Our work shows that the near future unambiguous detection of the global 21 cm absorption troughs can be an excellent probe of PBH DM.

DOI: 10.1103/PhysRevD.105.103026

I. INTRODUCTION

The prospect of detecting global 21 cm signal has been of interest for many years [1–5]. The early Universe, after recombination, was mostly filled with neutral hydrogen. The redshifted 21 cm line arising from the hyperfine splitting of the ground state of neutral hydrogen [4] can work as an important tracer to the temperature and ionization history of the intergalactic medium (IGM). From the astrophysical point of view, this can shed light on the exact epoch of reionization and the formation of earliest stars and galaxies [6–10]. It can also provide important insights into the cosmology and fundamental physics of the early Universe, especially of various beyond the Standard Model scenarios. Recently, the first possible and controversial observation of global 21 cm signal by the EDGES collaboration [11] has rejuvenated interest in this field. The collaboration has detected an absorption trough with differential brightness temperature, $T_{21} = -500^{+200}_{-500}$ mK at 78 MHz ($z \sim 17.2$) with 99% confidence level. The amplitude of this measured absorption trough is more than two times larger than the theoretical prediction from the Λ cold dark matter (ΛCDM) model of the Universe [4,12–15]. This has resulted in plethora of research on the origin of the anomaly [16–49]. The EDGES result has also stirred up a lot of controversy [50–54]. More recently, SARAS 3 has performed an independent check on this signal. SARAS 3 rejected EDGES signal with 95.3% confidence level [55]. In spite of this very recent development, we use the EDGES measurement in this paper as a representative of any global 21 cm excess that may potentially be observed in the near future.

The matter content of our present Universe is dominated by DM. The true nature of DM has been a mystery for a long time. Although we have detected the gravitational signatures of DM over a variety of length scales, we are yet to detect any other fundamental interaction of it [56–60]. Of all the DM candidates, PBHs are one of the oldest (see Ref. [61] for a historical review of DM and Refs. [62–67] for recent reviews on PBH DM). PBHs are formed from large density perturbations or from other exotic mechanisms in the early Universe (see for, e.g., [68–73]. Depending on their formation time [64], the mass of a PBH is thought to lie anywhere between Planck mass and few hundred solar masses. A PBH both Hawking radiates [74] and accretes, although Hawking emission dominates for low-mass PBHs (in this work, we will refer to PBHs in mass range 10^{15}–10^{18} g as low-mass PBHs). Accretion dominates for BHs with masses greater than a few solar mass [75]. Nonspinning PBHs with masses $\lesssim 6 \times 10^{14}$ g have evaporated by now [76,77]. Extensive work has been done regarding the search for evaporating PBHs as DM candidate from various astrophysical observables [78–98].

[*]akashks@iisc.ac.in
[†]ranjanlaha@iisc.ac.in

A low-mass PBH emits all sorts of particles, and these can subsequently heat up the IGM depending on particle interactions. As the amplitude of the absorption trough in a global 21 cm signal depends on the temperature and ionization of the IGM at a given redshift, if low-mass PBH DM exists, they can affect the observed global 21 cm signal.

Various authors have already considered similar ideas [99–107]. In this work, in order to constrain PBH DM, we consider the absorption troughs at redshift ∼17 (EDGES-like measurement) and the one expected at Dark Ages. The latter trough solely depends on the underlying cosmology and not on various astrophysical uncertainties. For the EDGES-like measurement, we consider excess background radiation and nonstandard recombination as explanations of the signal. In addition, we also consider the effects a power-law excess background radiation (which is consistent with EDGES-like signal) on the Dark Ages absorption trough.

We structure this paper as follows. In Sec. II we briefly review the underlying physics of 21 cm cosmology and the origin of both the absorption troughs. In Sec. III we discuss the standard thermal history of IGM in the absence of any exotic physics. In Sec. IV PBH evaporation is discussed in detail. In Sec. V we display our results, and we conclude in Sec. VI.

II. 21 CM COSMOLOGY

A 21 cm line is an important tool in modern astrophysics and cosmology. Due to the interaction of magnetic moments of electron and proton in neutral hydrogen, we have a splitting in the ground state energy level. The energy difference between the levels corresponds to a photon of frequency 1420 MHz or wavelength of around 21 cm. The global 21 cm signal is represented by the differential brightness temperature [108]

$$\delta T_b = T_{21} \approx x_{\rm HI}(z)\left(\frac{0.15}{\Omega_m}\right)^{1/2}\left(\frac{\Omega_b h}{0.02}\right) \times \left(\frac{1+z}{10}\right)^{1/2}\left(1-\frac{T_R(z)}{T_S(z)}\right)23\ \text{mK}, \quad (1)$$

where $x_{\rm HI}(z)$ is the neutral hydrogen fraction as a function of redshift z, Ω_m and Ω_b are the matter and baryon energy density parameter today, respectively, h is the current Hubble parameter in units of 100 $\text{km s}^{-1}\,\text{Mpc}^{-1}$, T_R is the background radiation temperature, and T_S is the spin temperature which is also known as 21 cm excitation temperature. T_S is defined as the ratio between the number densities (n_i) of hydrogen atoms in the two hyperfine levels

$$\frac{n_1}{n_0} = \frac{g_1}{g_0} e^{-T_*/T_S}, \quad (2)$$

where subscript 0 and 1 are for 1S singlet and triplet states, respectively. The ratio of statistical degeneracy factors of two levels is denoted by g_1/g_0 and $T_* = hc/k\lambda_{21\ \text{cm}} = 0.068$ K [4]. Spin temperature can also be written as

$$T_S^{-1} = \frac{T_R^{-1} + x_\alpha T_\alpha^{-1} + x_c T_K^{-1}}{1 + x_\alpha + x_c}, \quad (3)$$

where T_α and T_K are the color temperature of Lyman-α radiation field and gas kinetic temperature, respectively. The terms x_α, x_c are the coupling coefficients due to Lyman-α photon scattering and atomic collisions, respectively. Equation (1) implies that an absorption signal ($\delta T_b < 0$) requires $T_S < T_R$. Below we will briefly discuss the origin of two absorption troughs expected in the global 21 cm signal [4].

A. Dark Ages trough

After recombination, cosmic microwave background (CMB) temperature was coupled to the gas temperature (T_m) through Compton scattering with the residual free electrons, implying $T_m \approx T_R$ (assuming $T_R = T_{\rm CMB}$). On the other hand, collisions between neutral hydrogen atoms, free protons, and free electrons in the gas induced 21 cm transitions, which ensures $T_S \approx T_m$. The above two conditions imply $T_S \approx T_R$, which in turn results in $\delta T_b \approx 0$ from Eq. (1). Thus, we cannot have a 21 cm signal from this period. This Compton scattering with residual electrons is only efficient until $(1+z) \sim 155$. Afterwards due to adiabatic cooling, the gas temperature evolves as, $T_m \propto (1+z)^2$, thus falling faster than the CMB temperature, $T_{\rm CMB} \propto (1+z)$. This ensures that $T_m < T_R$. Collisional coupling still prevailed and as a result we get $T_S < T_R$ during this period. This results in $\delta T_b < 0$ and we have the first absorption trough at the Dark Ages ($35 \lesssim z \lesssim 200$). The absorption trough ends at the point where collisional coupling becomes ineffective (due to low density of gas) and radiative coupling with CMB ensures $T_S = T_R$.

B. Prereionization trough

As the first stars begin to form, the Lyman-α photons from them heat up the gas and create 21 cm transitions. Lyman-α photons can excite an atom in the ground state to any one of the excited states (depending on the selection rule) and the atom can later deexcite via emission of a Lyman-α photon. During deexcitation, the atom can return to either of the ground state hyperfine levels. If an atom initially at hyperfine singlet state (triplet state) returns later to the triplet state (singlet state), then spin flip transition occurs. Due to this Lyman-α coupling (Wouthuysen-Field effect [109,110]), we have $T_m \leq T_S < T_R$. This results in the second absorption trough. The depth of this trough depends on various uncertain astrophysical parameters [111,112]. EDGES has recently claimed a detection of this trough with $T_{21} = -500^{+200}_{-500}$ mK at redshift $z \sim 17.2$

with 99% confidence level, although SARAS 3 has rejected the claim at 95.3% confidence level. The end of this trough is marked by the saturation of the effect of Lyman-α coupling ($x_\alpha \gg 1$) and soon heating becomes effective. Due to heating once we have $T_m \approx T_R$, we do not have any further 21 cm absorption signal.

III. STANDARD THERMAL AND IONIZATION HISTORY

Before proceeding to the exotic heating due to PBHs, we first briefly review the standard thermal and ionization history. This is well described by the three-level atom model which simplifies the infinite energy levels of hydrogen atom into three levels—ground state ($n = 0$), first excited state ($n = 1$), and continuum state ($n = \infty$) [113,114]. The temperature and ionization evolution can be described the following differential equations [17]

$$\frac{dT_m^{(0)}}{dt} = -2HT_m^{(0)} + \Gamma_c(T_{\rm CMB} - T_m^{(0)}), \tag{4}$$

$$\frac{dx_e^{(0)}}{dt} = -\mathcal{C}\left[n_H (x_e^{(0)})^2 \alpha_B - 4(1 - x_e^{(0)})\beta_B e^{\frac{-E_{21}}{T_{\rm CMB}}}\right]. \tag{5}$$

Here $T_m^{(0)}$ is the standard gas temperature, t denotes time, H is the Hubble parameter, Γ_c is the Compton scattering rate, $T_{\rm CMB}$ is the CMB temperature, $x_e^{(0)} = n_e/n_H$, where n_e, n_H are the number densities of free electrons and hydrogen atoms, respectively. The Peebles-C factor is denoted by $\mathcal{C}$, α_B, β_B are the case-B recombination and photoionization coefficients, and $E_{21} = 10.2$ eV is the Lyman-α transition energy. The Compton scattering rate (Γ_c) is given by

$$\Gamma_c = \frac{x_e^{(0)}}{1 + f_{\rm He} + x_e^{(0)}} \frac{8\sigma_T a_r T_{\rm CMB}^4}{3 m_e c}, \tag{6}$$

where $f_{\rm He} = n_{\rm He}/n_H$ is the relative abundance of helium nuclei by number, σ_T is the Thomson cross section, a_r is the radiation constant, and m_e is the electron mass. In the presence of exotic heating due to new physics, both Eqs. (4) and (5) get modified.

IV. EVAPORATION OF NONSPINNING AND SPINNING PBH

The temperature of an uncharged, spinning PBH is given by [76,115,116]

$$T_{\rm PBH} = \frac{\hbar c^3}{4\pi G M_{\rm PBH}} \left(\frac{\sqrt{1 - a_*^2}}{1 + \sqrt{1 - a_*^2}}\right), \tag{7}$$

where $\hbar$ is the reduced Planck's constant, c is the speed of light, G is the gravitational constant, $M_{\rm PBH}$ is the mass of the PBH and

$$a_* = \frac{c^4 J}{G M_{\rm PBH}^2}, \tag{8}$$

with a_* being the reduced spin parameter, and J is the magnitude of angular momentum of the PBH. For $a_* \to 0$, from Eq. (7) we get the temperature of the uncharged, nonspinning PBH [116] as

$$T_{\rm PBH} = \frac{\hbar c^3}{8\pi G M_{\rm PBH}} = 1.06 \left(\frac{10^{13}\ {\rm g}}{M_{\rm PBH}}\right) {\rm GeV}. \tag{9}$$

Throughout our analysis we assume uncharged PBHs. A charged low-mass PBH can discharge through pair production and it will have very little effect on the Hawking emission. Charge will only be an important parameter for PBHs with masses $\gtrsim 10^5\ M_\odot$ [76,117,118].

For primary emission, the number of particles, N_i emitted per unit energy per unit time is given by [76,115,116]

$$\frac{d^2 N_i}{dE dt} = \frac{1}{2\pi\hbar} \sum_{\rm dof} \frac{\Gamma_i(E, M_{\rm PBH}, a_*)}{e^{E'/kT} \pm 1}, \tag{10}$$

where Γ_i is the graybody factor [76,115,116] which encodes the probability of an emitted particle surpassing the gravitational potential of a PBH and E' is the total energy of the emitted particles taking into account the rotational velocity of the PBH.

For this work, we have used BLACKHAWKv2.0 [117,118] for the spectra of particles emitted from both nonspinning and spinning PBHs. For both non-spinning and spinning PBHs we have extensively checked the output obtained from BLACKHAWK with the analytical forms of graybody factor given in Ref. [76]. Both primary and secondary emissions can be taken into account, though there is some uncertainty in obtaining the secondary spectrum below a certain energy range. BLACKHAWKv2.0 has improved on the calculation of secondary emission. We only utilized the primary emission in this work as to keep the bounds conservative. The difference in constraints with using the secondary emission is at most 60% at the mass range $\sim 10^{15}$–10^{17} g. As a result of being created at a very early stage of the Universe, low-mass PBHs have the potential of having a significant effect on the thermal and ionization history by means of evaporation and subsequent energy injection into the cosmic plasma. In general, the deposited energy is related to the injected energy from Hawking emission of PBH by [17]

$$\left(\frac{dE}{dV dt}\right)_{\rm dep} = f_c(z) \left(\frac{dE}{dV dt}\right)_{\rm inj}, \tag{11}$$

where dV is the volume element and $f_c(z)$ is the deposition efficiency into energy deposition channel c at a given redshift z [119–121]. Photons, electrons, and positrons emitted from a low-mass PBH heat up and ionize the IGM

significantly. Here we consider energy deposition through hydrogen ionization ($f_{\rm ion}$), helium ionization ($f_{\rm He}$), hydrogen excitation ($f_{\rm exc}$) and heating of IGM ($f_{\rm heat}$). The energy deposited per unit volume per unit time by PBH of mass $M_{\rm PBH}$ and spin parameter a_* is given by

$$\left(\frac{dE}{dVdt}\right)_{\rm dep} = \left(\frac{dE}{dVdt}\right)^{\gamma}_{\rm dep} + \left(\frac{dE}{dVdt}\right)^{e^{\pm}}_{\rm dep}, \quad (12)$$

with

$$\left(\frac{dE}{dVdt}\right)^{\gamma}_{\rm dep} = \int\int f_c(E_\gamma, z) E_\gamma \left(\frac{d^2N}{dEdt}\right)_\gamma \times n_{\rm PBH}(M_{\rm PBH})\psi(M_{\rm PBH})dM_{\rm PBH}dE, \quad (13)$$

and

$$\left(\frac{dE}{dVdt}\right)^{e^{\pm}}_{\rm dep} = \int\int 2f_c(E_e - m_e c^2, z)(E_e - m_e c^2) \times \left(\frac{d^2N}{dEdt}\right)_{e^{\pm}} n_{\rm PBH}(M_{\rm PBH})\psi(M_{\rm PBH})dM_{\rm PBH}dE. \quad (14)$$

In the above equations, $n_{\rm PBH}$ is the number density of PBHs, $\psi(M_{\rm PBH})$ is the mass distribution function of the PBH. Here $n_{\rm PBH}$ can be written as

$$n_{\rm PBH} = f_{\rm PBH}\frac{\rho_c \Omega_{\rm DM}}{M_{\rm PBH}}, \quad (15)$$

where $f_{\rm PBH}$ is the fraction of DM in the form of PBHs, ρ_c and $\Omega_{\rm DM}$ are the critical density and DM density parameter in the present Universe. DARKHISTORY [122] has implemented $f_c(z)$ s that have been computed in Refs. [119–121]. For our work, we have used monochromatic mass distribution, but a discussion of extended mass distribution can be followed similarly.

The resulting modification in the temperature and ionization history due to emission from PBH can be computed from the following differential equations [17]:

$$\frac{dT_m}{dt} = \frac{dT_m^{(0)}}{dt} + \frac{dT_m^{\rm PBH}}{dt}, \quad (16)$$

$$\frac{dx_e}{dt} = \frac{dx_e^{(0)}}{dt} + \frac{dx_e^{\rm PBH}}{dt}, \quad (17)$$

where

$$\frac{dT_m^{\rm PBH}}{dt} = \frac{2f_{\rm heat}(z)}{3(1+f_{\rm He}+x_e)n_H}\left(\frac{dE}{dVdt}\right)_{\rm inj}, \quad (18)$$

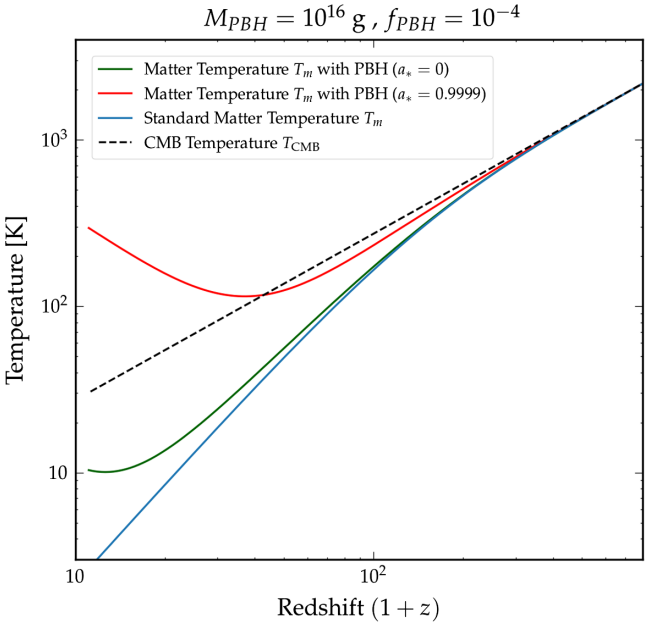

FIG. 1. Thermal history of IGM in the absence and presence of PBH DM with masses = 10^{16} g (monochromatic distribution) and $f_{\rm PBH} = 10^{-4}$. Here the temperature evolution of CMB (black dotted line) and standard matter temperature evolution (blue line) are shown in comparison with matter temperature evolution in the presence of nonspinning (green line) and spinning (red line) PBH DM.

$$\frac{dx_e^{\rm PBH}}{dt} = \left[\frac{f_{\rm ion}(z)}{\mathcal{R}n_H} + \frac{(1-\mathcal{C})f_{\rm exc}(z)}{0.75\mathcal{R}n_H}\right]\left(\frac{dE}{dVdt}\right)_{\rm inj}. \quad (19)$$

In the above equations $\mathcal{R}$ is the ionization potential of hydrogen. In presence of low-mass nonspinning and spinning PBH, the evolution of gas temperature as a function of redshift is shown in Fig. 1. As we can see in the figure, due to the presence of PBH, the IGM temperature increases significantly. The rate of emission of particles increases with the spin of the PBH. As a result, we see an increase in the gas temperature for spinning PBH with respect to the scenario with nonspinning PBH.

V. RESULTS

In this section, we describe all the results from this work in detail. In our redshift ranges of interest, $T_m(z) \lesssim T_S(z)$. Inverting Eq. (1) we can find $T_S(z)$ in terms of other variables. Combining these two relations, we get the bound on the gas temperature (T_m) from global 21 cm absorption troughs at a particular redshift as

$$T_m(z) \lesssim T_S(z) \sim x_{HI}\left(1 - \frac{0.12}{\sqrt{1+z}}T_{21}(z)\right)^{-1} T_R(z)\,\text{K}. \quad (20)$$

In presence of exotic heating, we will get a particular value of $T_m(z)$ by solving Eqs. (16) and (17). Since the amount of

exotic heating depends on $f_{\rm PBH}$, using the $T_m(z)$ bound obtained above, we can set upper bounds on $f_{\rm PBH}$ as a function of $M_{\rm PBH}$. In this work, we use the publicly available codes DARKHISTORY [122] and TWENTYONE-GLOBAL [123] to obtain our results. DARKHISTORY is used for the analysis of both standard and exotic energy injection and their subsequent effect on the temperature and ionization history of IGM. We use TWENTYONE-GLOBAL for obtaining both the standard 21 cm absorption troughs and the effect of power law radio excess on the trough at Dark Ages.

In Secs. V A and V B, we discuss the sensitivities on PBH DM coming from the prereionization and Dark Ages trough, respectively. Here for the prereionization trough, we use the differential brightness temperature measured by EDGES, along with the error bars ($T_{21} = -500^{+200}_{-500}$ mK). Standard cosmology cannot explain an EDGES-like signal. Following the approach taken by Ref. [17], we assume that either excess radiation at redshift $\sim$17.2 with respect to $T_{\rm CMB}$ or nonstandard recombination can explain an EDGES-like signal. Under these assumptions, we derive sensitivities on nonspinning ($a_* = 0$) and spinning ($a_* = 0.9999$) PBH DM. In Sec. V C, we discuss the effect of a power law radio excess on both the absorption troughs and the respective sensitivities on PBH DM.

A. Sensitivities from the prereionization trough (EDGES-like measurement)

1. Excess background radiation

From Eq. (1), we see that, for a fixed value of T_S, an increase in T_R can decrease the value of T_{21}. Measurements from ARCADE2 [124] and LWA1 [125] indicate an excess diffuse radio background in the frequency ranges 3–90 GHz and 40–80 MHz, respectively. If confirmed, then an excess background radiation can affect the 21 cm absorption trough and possibly explain an EDGES-like result [14,19]. A power law form for the excess background radiation consistent with these measurements will be discussed later.

In this section, we remain agnostic of the origin of this excess background radiation and instead use a model independent way of considering excess radiation. We parametrize the excess radio background by taking it to be an integer multiple of the CMB temperature at the redshift of interest. Figure 2 shows sensitivities on nonspinning ($a_* = 0$) and spinning ($a_* = 0.9999$) PBH DM, respectively, assuming $T_R = 5T_{\rm CMB}$.

The sensitivities on spinning PBH DM are more stringent compared to nonspinning PBH DM due to the increased rate in emission of particles. In the same figures,

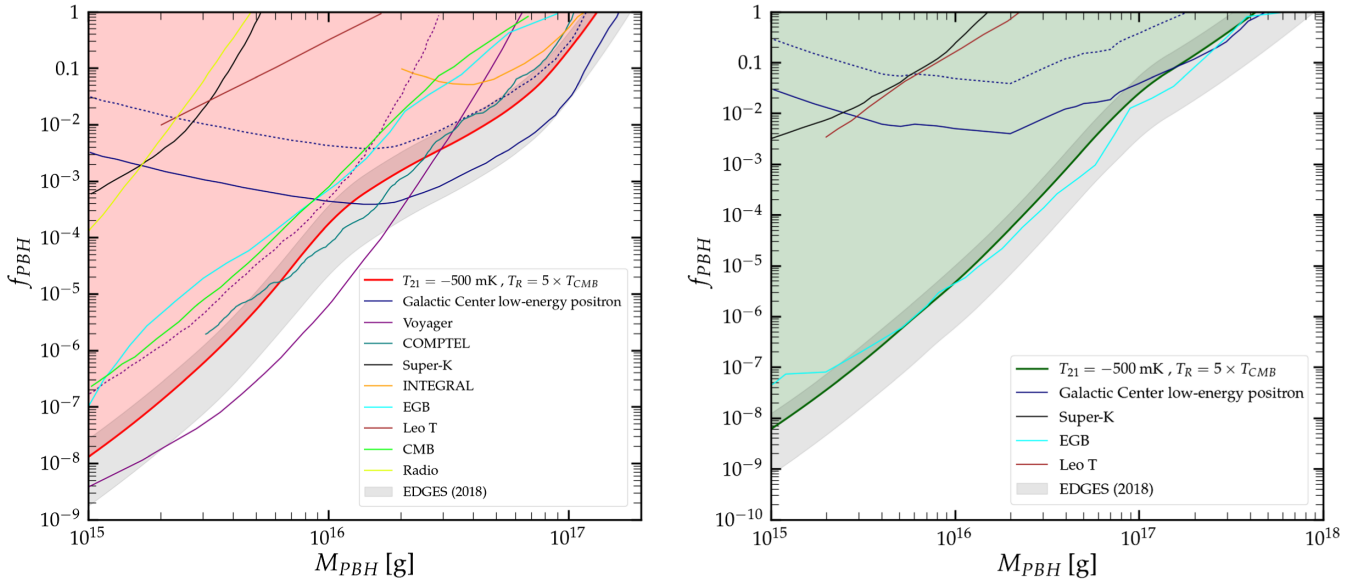

FIG. 2. Sensitivities on nonspinning ($a_* = 0$) and spinning ($a_* = 0.9999$) PBH DM (monochromatic distribution) from an assumed 21 cm absorption trough, similar to the one detected by EDGES ($T_{21} = -500^{+200}_{-500}$ mK), shown by the red (left panel) and green (right panel) lines, respectively. For these limits, we assume $T_R = 5T_{\rm CMB}$ ($z = 17.2$). The gray shaded regions show the impact of the EDGES measurement uncertainty. Previous constraints include Galactic Center low-energy positron measurements by INTEGRAL (navy dotted line for isothermal with 1.5 kpc and navy continuous line for Navarro-Frenk-White (NFW) with 3.5 kpc region of interest) [81], measurement of the cosmic-ray flux by Voyager (purple dotted line for propagation model B without background and purple continuous line for propagation model A with background) [82], COMPTEL (teal), and INTEGRAL (orange) measurements of the Galactic Center keV-MeV gamma-ray flux [78,83], Super-Kamiokande search for diffuse supernovae neutrino background (black) [84], extra-Galactic gamma-ray emission measurement (aqua) [85,126], Leo T gas heating (brown) [86] (see however Ref. [127]), measurement of CMB from PLANCK (lime) [87], and radio measurement of the inner Galactic Center (NFW profile) (lemon lime) [89]. Some of the constraints for nonspinning PBH DM are absent for spinning PBH DM because they are not present in the literature.

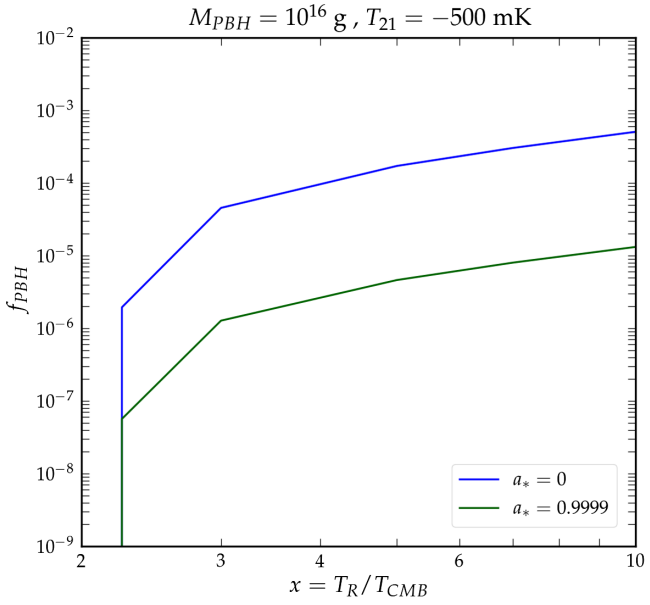

FIG. 3. EDGES-like ($T_{21} = -500^{+200}_{-500}$ mK) measurement sensitivities on nonspinning ($a_* = 0$) and spinning ($a_* = 0.9999$) PBH DM (monochromatic distribution) of mass 10^{16} g as a function of excess radiation given as integer multiples of $T_{\rm CMB}$ at redshift of interest ($z = 17.2$).

we also show the previous constraints [78,81–87,89,127] on low-mass PBH DM. In Fig. 3, we show the dependence of sensitivities on different background radiation T_R, which is taken as multiples of $T_{\rm CMB}(z = 17.2)$ for PBH DM with mass 10^{16} g. As we increase the background radiation, the allowed upper limit on $T_m(z)$ increases. Thus, for a fixed $M_{\rm PBH}$ the allowed $f_{\rm PBH}$ increases and as a result the respective sensitivities become weaker. We notice that there is a cutoff in this plot. This is because, below a certain value of excess T_R, the value of required T_m to explain EDGES-like result falls below the standard IGM gas temperature at $z \sim 17.2$.

Following the discussion of Fig. 3, we realise that sensitivities in Fig. 2 can be considerably strengthened for $2.2T_{\rm CMB} < T_R < 5T_{\rm CMB}$. As a result, the sensitivities from this work can extend to some new regions of the parameter space, beyond the reach of the current constraints. We emphasize that these values of excess radiation are not actual measurements, but are taken to demonstrate the dependence of the sensitivities on the excess background radiation required to explain an EDGES-like result.

2. Nonstandard recombination

During prereionization, $T_m \leq T_S$ and from Eq. (1) we see that, a cooler than expected T_m can decrease T_{21} and can potentially also explain an EDGES-like signal. Various mechanisms for the exotic cooling of gas at this epoch, have been explored in the literature. Some of them are DM-baryon scattering [17,128,129], charge sequestration [28] and influence of early dark energy [130]. The last two scenarios work via altering the redshift of thermal decoupling to a larger value, implying that $T_m(z)$ evolves as $(1+z)^2$ for a longer duration, and it can possibly explain an EDGES-like excess.

We take the approach of Ref. [17] and parametrize the early redshift of thermal decoupling as $(1+z)_{td}$. We show the sensitivities on nonspinning and spinning PBH DM

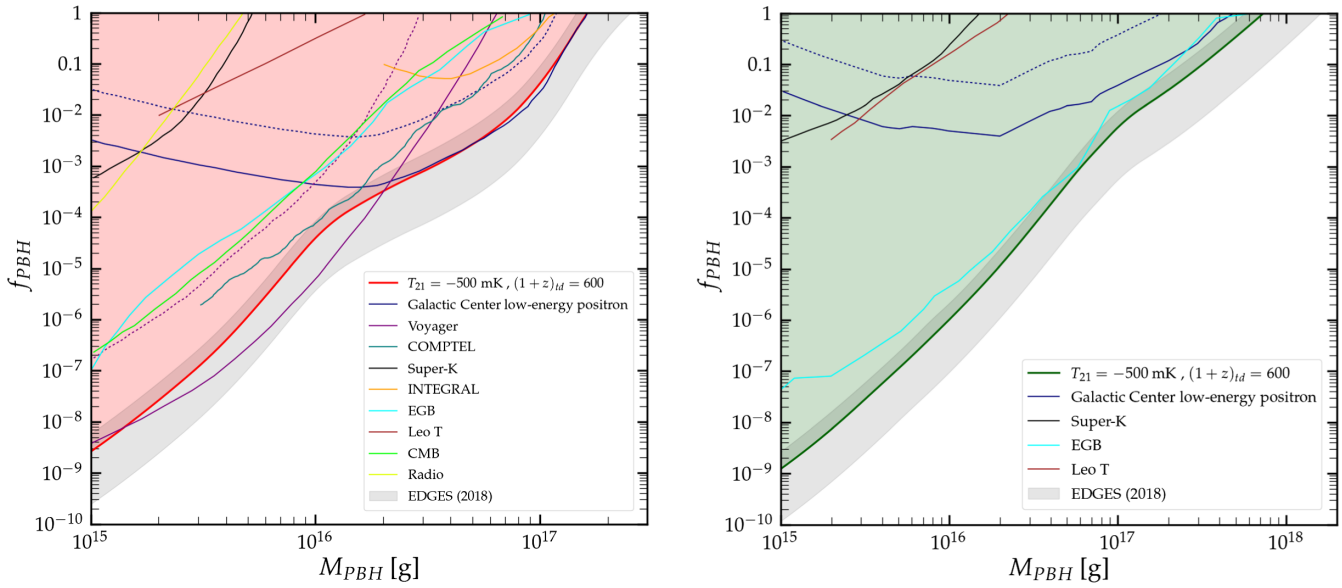

FIG. 4. Sensitivities on nonspinning ($a_* = 0$) and spinning ($a_* = 0.9999$) PBH DM (monochromatic distribution) from an assumed 21 cm absorption trough, similar to the one detected by EDGES ($T_{21} = -500^{+200}_{-500}$ mK), shown by the red (left panel) and green (right panel) lines, respectively. For these limits, we assume $(1+z)_{td} = 600$. The gray shaded regions show the impact of the EDGES measurement uncertainty. Previous constraints are shown as mentioned before.

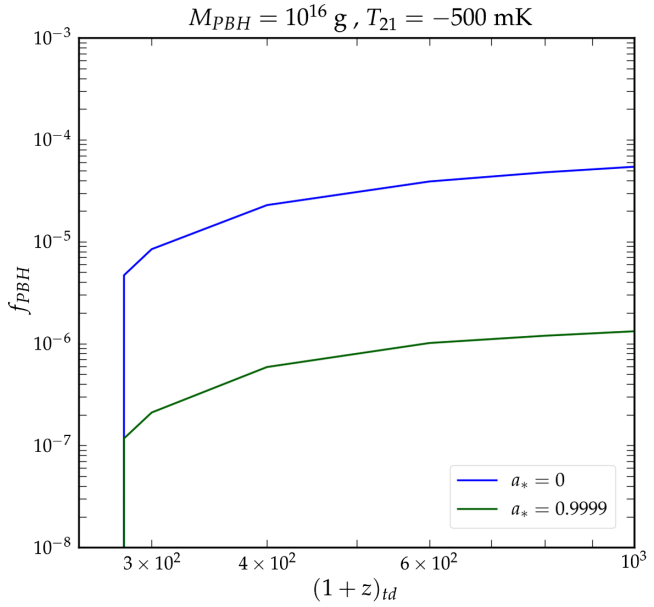

FIG. 5. EDGES-like ($T_{21} = -500^{+200}_{-500}$ mK) measurement sensitivities on both nonspinning ($a_* = 0$) and spinning ($a_* = 0.9999$) PBH DM (monochromatic distribution) of mass 10^{16} g as a function of the redshift of thermal decoupling $(1+z)_{td}$.

from an EDGES-like signal in Fig. 4 assuming $(1+z)_{td} = 600$, along with constraints from other observables.

In Fig. 5, we show the dependence of the sensitivities on the redshift of thermal decoupling for PBH DM with mass 10^{16} g. As we increase $(1+z)_{td}$ for a fixed mass of PBH, the gas temperature keeps on decreasing and this allows a larger fraction of PBH (as DM) to be present. Thus the corresponding sensitivities become weaker. After $(1+z)_{td}$ exceeds a critical value for sufficient cooling, the dependence of sensitivities on redshift of thermal decoupling is rather weak, as can be seen in the figure. As we decrease $(1+z)_{td}$, the allowed upper limit on $T_m(z)$ decreases. Thus, for a fixed $M_{\rm PBH}$ the allowed $f_{\rm PBH}$ decreases and the sensitivities become stronger. Here our choice of $(1+z)_{td} = 600$ and the respective sensitivities are conservative.

If future experiments measure differential brightness temperature (T_{21}) in agreement with standard astrophysical expectations [131–137], then constraints on PBH DM can be derived without any additional assumption. In Fig. 6, we show the sensitivities on nonspinning and spinning PBH DM due to a range of standard T_{21} (for redshift $\sim$17.2), consistent with [134]. As we decrease the value of T_{21} (more negative), the bounds on gas temperature get tighter [from Eq. (20)], and with that the bounds on $f_{\rm PBH}$ get stronger.

B. Projections of constraints from the Dark Ages trough

Similar to the prereionization trough, another 21 cm absorption trough is expected during the Dark Ages. Various astrophysical uncertainties do not contribute to the amplitude of this absorption trough unlike the prereionozation trough, though there are less severe uncertainties from the values of the cosmological parameters [14]. In many cases, deviations from the standard ΛCDM predictions of the prereionization trough can also affect the Dark Ages trough (one such example will be discussed later). Detection of any deviation from the standard Dark Ages trough will directly point towards new physics and can potentially probe the nature of DM. Future space-based

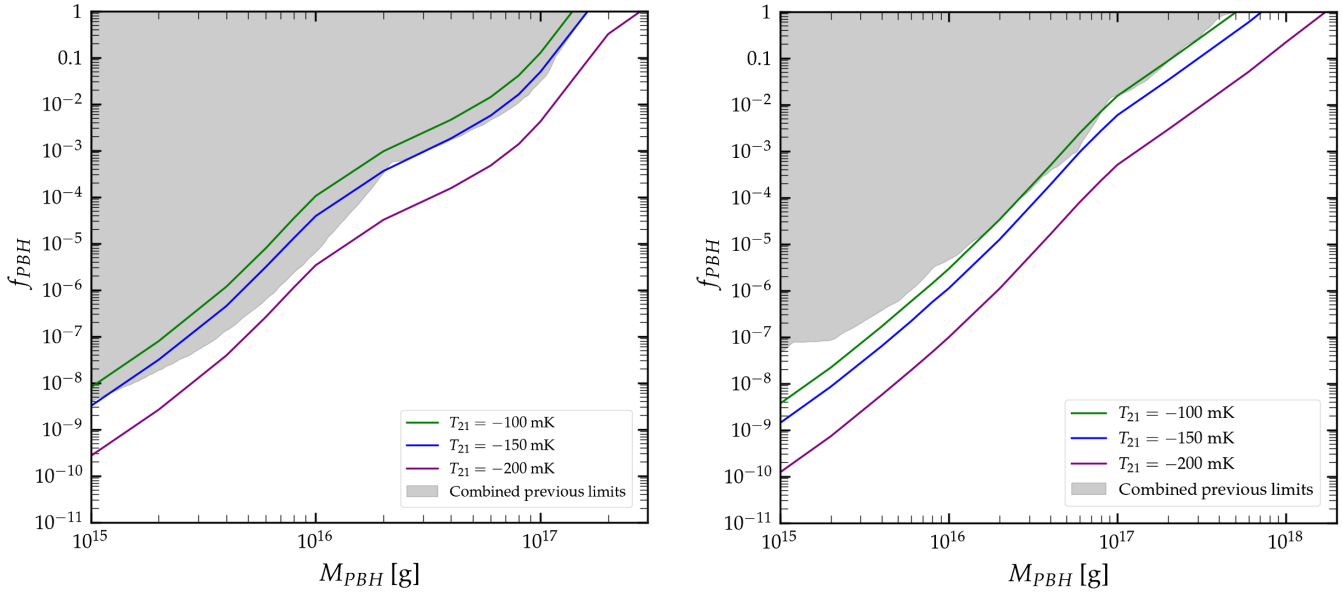

FIG. 6. Sensitivities on nonspinning ($a_* = 0$) and spinning ($a_* = 0.9999$) PBH DM (monochromatic distribution) arising from the prereionization trough with different values of differential brightness temperature (T_{21}), shown in left and right panels, respectively. The black shaded regions show combined previous limits as mentioned before.

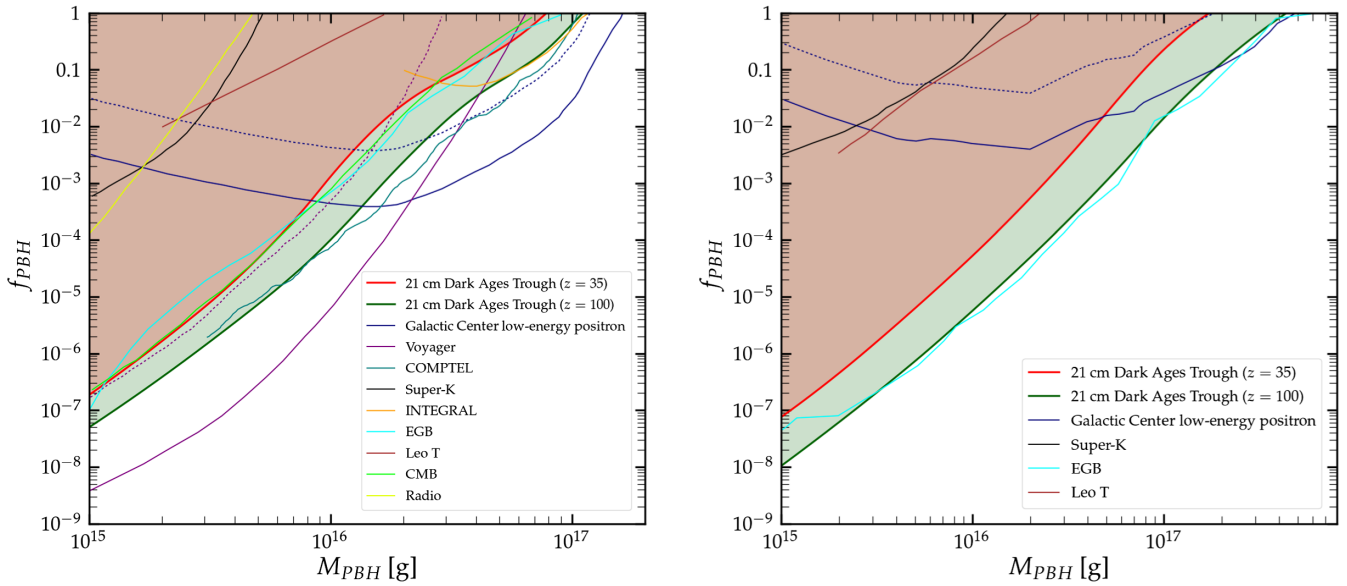

FIG. 7. Projections of constraints on nonspinning ($a_* = 0$) and spinning ($a_* = 0.9999$) PBH DM (monochromatic distribution) arising from Dark Ages absorption trough ($z = 35$–100), due to standard cosmology, shown in left and right panels respectively. Previous constraints are shown as mentioned before.

detectors like DAPPER [138], FARSIDE [139], DSL [140], and NCLE [141] will be able to probe this signal.

For this trough, we obtain the value of standard $T_{21}(z)$ using TWENTYONE-GLOBAL [123] and then use Eq. (20) to find an upper bound on $T_m(z)$. With this upper bound, we use DARKHISTORY [122] to solve Eqs. (16) and (17) to obtain the upper bound on $f_{\rm PBH}$ as a function of $M_{\rm PBH}$. We show the projections of constraints on nonspinning and spinning PBH DM from the Dark Ages trough, expected due to standard cosmology in Fig. 7 ($z = 35$–100). At higher redshifts, the increased density of PBH DM can significantly heat up the gas. Thus one expects stronger constraints from this trough. But due to the interplay between lower T_{21} and higher T_R ($T_{\rm CMB}$), one does not get a strong limit. These projected constraints from Dark Ages trough can be strengthened if we use measurement uncertainties assuming that the signal follows the standard ΛCDM predictions. Any constraint from the prereionization trough will be affected by astrophysical uncertainties unless we substantially improve both theoretical and experimental understanding of this signal. In contrast, the Dark Ages trough has much less astrophysical uncertainties, and thus is the more conservative way of probing DM in general.

C. Effect of power law radio excess on the absorption troughs

We have previously discussed the scenario with excess radio background and the sensitivities on PBH arising from that. Here we try to investigate the effect of a power law radio excess consistent with measurements from ARCADE2 [124] and LWA1 [125]. The phenomenological power law is given by [14]

$$T_{\rm rad}(z) = T_{\rm CMB,0}(1+z)\left[1 + A_r\left(\frac{\nu_{\rm obs}}{78\ {\rm MHz}}\right)^{\beta}\right], \quad (21)$$

where $T_{\rm rad}$ is the radio background at any given redshift z and $T_{\rm CMB,0}$ is the CMB temperature today (= 2.7 K), A_r is the amplitude defined relative to the CMB temperature, $\nu_{\rm obs}$ is the observed photon frequency and β is the spectral index. The modified radio background has significant effect

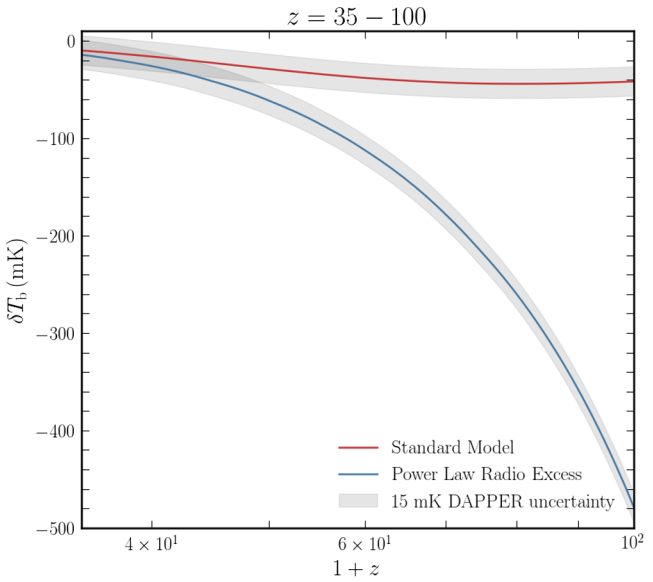

FIG. 8. Differential brightness temperature expected from standard cosmology (red line) and with a power law excess background radiation with $A_r = 5.7$ and $\beta = -2.6$ (blue line). The shaded region shows 15 mK DAPPER uncertainty in T_{21} measurement [138].

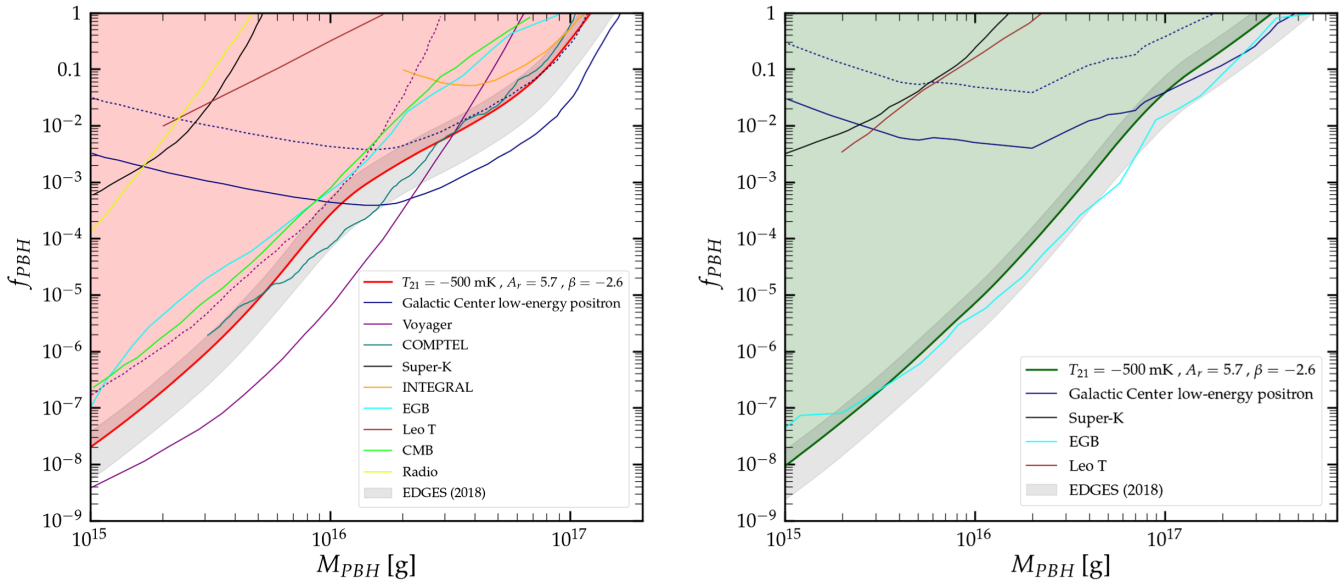

FIG. 9. Sensitivities on nonspinning ($a_* = 0$) and spinning ($a_* = 0.9999$) PBH DM (monochromatic distribution) from an assumed 21 cm absorption trough, similar to the one detected by EDGES ($T_{21} = -500^{+200}_{-500}$ mK), shown in left and right panels, respectively. Here we assume power law radio excess ($A_r = 5.7, \beta = -2.6$) consistent with an EDGES-like result. Previous constraints are shown as mentioned before.

on the differential brightness temperature both at prereionization and Dark Ages trough. This effect is shown in Fig. 8 for the values of $A_r = 5.7$ and $\beta = -2.6$ (one of the example parameters used in [14]). We also show the 15 mK DAPPER uncertainty within the same plot [138].

If we consider EDGES-like excess at the prereionization trough and if this occurs solely due to the power law excess radiation, then the signature must be there in the Dark Ages trough also. We use TWENTYONE-GLOBAL to get the modified $T_{21}(z)$, assuming the radiation temperature is given by Eq. (21). Using Eq. (20), we get the bound on $T_m(z)$. The upper bound on $T_m(z)$ is used to obtain the bounds on $f_{\rm PBH}$ using DARKHISTORY.

In Fig. 9, we show the sensitivities arising from the power law excess radiation ($A_r = 5.7$ and $\beta = -2.6$) at the prereionization trough on both nonspinning and spinning

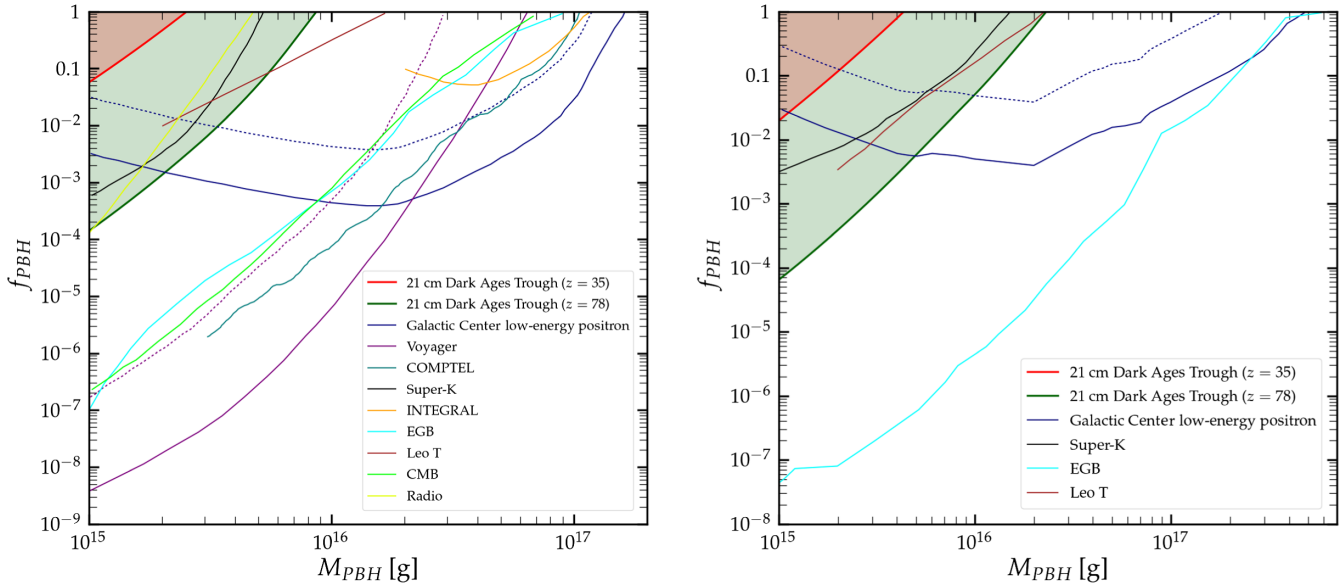

FIG. 10. Projections of constraints on nonspinning ($a_* = 0$) and spinning ($a_* = 0.9999$) PBH DM (monochromatic distribution) arising from Dark Ages absorption trough ($z = 35$–78), shown in left and right panels, respectively. Here we assume power law radio excess ($A_r = 5.7$, $\beta = -2.6$) consistent with an EDGES-like result. Previous constraints are shown as mentioned before.

PBH, respectively, considering an EDGES-like result ($T_{21} = -500^{+200}_{-500}$ mK). Similarly in Fig. 10, we show the projections of constraints on nonspinning and spinning PBH, respectively, considering the modified Dark Ages trough with excess power law radiation consistent with an EDGES-like excess. The upper limits are shown for redshift, $z = 35$–78 which is within the projected redshift in which DAPPER will operate [138]. We see that, at higher redshifts, the projections of constraints on both nonspinning and spinning PBHs are getting weaker as the effect of excess background is getting stronger (see Fig. 8). In the left panel of Fig. 1 from Ref. [14] we see that effect of different values for parameters A_r and β saturate at Dark Ages. Hence, here also the projected upper limits from Dark Ages have very weak dependence on the value of the excess radio background parameters and are thus conservative. In future, detection of the Dark Ages absorption trough will be a good test for the verification of a power law radio excess consistent with ARCADE and LWA1.

All the upper limits shown are obtained without taking the effect of backreaction. The effect of backreaction changes the sensitivities between 8 to 30%. Besides, there are various possible reionization models which can strengthen the sensitivities. We did not take any particular reionization model, as a result of which all of our sensitivities are conservative.

VI. CONCLUSION

In this work, we derive sensitivities and projections on both nonspinning and spinning PBH DM from prereionization and Dark Ages absorption troughs expected in the global 21 cm signal, respectively. Recently EDGES collaboration has claimed a detection of this prereionization trough, though more recently SARAS 3 has rejected this detection. Our work explores the bounds expected from any future detection of global 21 cm excess similar to that of EDGES. For prereionization trough, we use the EDGES signal as the benchmark and derive conservative sensitivities assuming two scenarios, i.e., excess background radiation (at $z \sim 17.2$) and nonstandard recombination. These limits are comparable with existing limits. Our limits can be significantly strengthened by taking slightly lower value of excess radiation temperature and higher redshift of thermal decoupling. We also consider the scenario where future measurement of global 21 cm prereionization trough yields a differential brightness temperature that is within the standard astrophysical expectation. Using that we derive the corresponding constraints on PBH DM and notice that for lower values of T_{21} we can probe new parts of PBH DM parameter space. For the Dark Ages trough, we use the absorption trough expected from standard ΛCDM model to obtain our projections. Later we discuss the possibility of a power law excess radiation hinted by both ARCADE and LWA1 measurements. We derive sensitivities on $f_{\rm PBH}$ from an EDGES-like signal and Dark Ages trough in the presence of such excess power-law background radiation. The Dark Ages trough is still beyond the reach of current global 21 cm signal detectors, but in the future, space-based telescopes will be able to detect such signal. A combined detection of both the absorption troughs will in future provide the best insight to the Universe during both Dark Ages and Cosmic Dawn, and using these measurements one can either discover or constrain various well motivated beyond Standard Model physics scenarios. In addition to various near-future 21 cm experiments, low-mass PBH DM can also be discovered by various upcoming neutrino, low-energy gamma-ray, cosmic ray, CMB, radio experiments and measurements sensitive to Galactic Center low-energy positrons [83,142–150]. A combination of all of these experiments will fully explore the low-mass PBH DM parameter space.

ACKNOWLEDGMENTS

We especially thank Hongwan Liu for detailed help regarding DARKHISTORY, and also for his comments on the manuscript. We also thank Julian B. Muñoz, Tarak Nath Maity, and Shikhar Mittal for their useful comments and suggestions. R. L. acknowledges financial support from the Infosys foundation, Bangalore and institute start-up funds.

Note added.—References [105–107] appeared in arXiv while this work was in preparation.

[1] S. Furlanetto *et al.*, Astro 2020 science white paper: Fundamental cosmology in the dark ages with 21-cm line fluctuations, arXiv:1903.06212.
[2] S. Furlanetto *et al.*, Astro2020 science white paper: Insights into the epoch of reionization with the highly-redshifted 21-cm line, arXiv:1903.06204.
[3] A. Liu *et al.*, Cosmology with the highly redshifted 21 cm line, arXiv:1903.06240.
[4] J. R. Pritchard and A. Loeb, 21 cm cosmology in the 21st century, Rep. Prog. Phys. **75**, 086901 (2012).
[5] H. Padmanabhan, A multi-messenger view of cosmic dawn: Conquering the final frontier, Int. J. Mod. Phys. D **30**, 2130009 (2021).
[6] J. Mirocha and S. R. Furlanetto, What does the first highly-redshifted 21-cm detection tell us about early galaxies?, Mon. Not. R. Astron. Soc. **483**, 1980 (2019).

[7] J. Park, A. Mesinger, B. Greig, and N. Gillet, Inferring the astrophysics of reionization and cosmic dawn from galaxy luminosity functions and the 21-cm signal, Mon. Not. R. Astron. Soc. **484**, 933 (2019).
[8] J. B. Muñoz, C. Dvorkin, and F.-Y. Cyr-Racine, Probing the small-scale matter power spectrum with large-scale 21-cm data, Phys. Rev. D **101**, 063526 (2020).
[9] J. B. Muñoz, Y. Qin, A. Mesinger, S. G. Murray, B. Greig, and C. Mason, The impact of the first galaxies on cosmic dawn and reionization, Mon. Not. R. Astron. Soc. **511**, 3657 (2022).
[10] M. Magg, I. Reis, A. Fialkov, R. Barkana, R. S. Klessen, S. C. O. Glover *et al.*, Effect of the cosmological transition to metal-enriched star-formation on the hydrogen 21-cm signal, arXiv:2110.15948.
[11] J. D. Bowman, A. E. E. Rogers, R. A. Monsalve, T. J. Mozdzen, and N. Mahesh, An absorption profile centred at 78 megahertz in the sky-averaged spectrum, Nature (London) **555**, 67 (2018).
[12] Y. Ali-Haïmoud and C. M. Hirata, Hyrec: A fast and highly accurate primordial hydrogen and helium recombination code, Phys. Rev. D **83**, 043513 (2011).
[13] J. Chluba and R. M. Thomas, Towards a complete treatment of the cosmological recombination problem, Mon. Not. R. Astron. Soc. **412**, 748 (2011).
[14] A. Fialkov and R. Barkana, Signature of excess radio background in the 21-cm global signal and power spectrum, Mon. Not. R. Astron. Soc. **486**, 1763 (2019).
[15] Y. Xu, B. Yue, and X. Chen, Maximum absorption of the global 21 cm spectrum in the standard cosmological model, Astrophys. J. **923**, 98 (2021).
[16] S. Fraser *et al.*, The EDGES 21 cm anomaly and properties of dark matter, Phys. Lett. B **785**, 159 (2018).
[17] H. Liu and T. R. Slatyer, Implications of a 21-cm signal for dark matter annihilation and decay, Phys. Rev. D **98**, 023501 (2018).
[18] R. Barkana, N. J. Outmezguine, D. Redigolo, and T. Volansky, Strong constraints on light dark matter interpretation of the EDGES signal, Phys. Rev. D **98**, 103005 (2018).
[19] C. Feng and G. Holder, Enhanced global signal of neutral hydrogen due to excess radiation at cosmic dawn, Astrophys. J. Lett. **858**, L17 (2018).
[20] A. Ewall-Wice, T. C. Chang, J. Lazio, O. Dore, M. Seiffert, and R. A. Monsalve, Modeling the radio background from the first black holes at cosmic dawn: Implications for the 21 cm absorption amplitude, Astrophys. J. **868**, 63 (2018).
[21] J. B. Muñoz and A. Loeb, A small amount of mini-charged dark matter could cool the baryons in the early Universe, Nature (London) **557**, 684 (2018).
[22] A. Fialkov, R. Barkana, and A. Cohen, Constraining Baryon–Dark Matter Scattering with the Cosmic Dawn 21-cm Signal, Phys. Rev. Lett. **121**, 011101 (2018).
[23] S. McGaugh, Strong hydrogen absorption at cosmic dawn: The signature of a baryonic universe, Res. Notes AAS **2**, 37 (2018).
[24] A. Berlin, D. Hooper, G. Krnjaic, and S. D. McDermott, Severely Constraining Dark Matter Interpretations of the 21-cm Anomaly, Phys. Rev. Lett. **121**, 011102 (2018).
[25] Y. Yang, Contributions of dark matter annihilation to the global 21 cm spectrum observed by the EDGES experiment, Phys. Rev. D **98**, 103503 (2018).
[26] M. Pospelov, J. Pradler, J. T. Ruderman, and A. Urbano, Room for New Physics in the Rayleigh-Jeans Tail of the Cosmic Microwave Background, Phys. Rev. Lett. **121**, 031103 (2018).
[27] A. A. Costa, R. C. G. Landim, B. Wang, and E. Abdalla, Interacting dark energy: Possible explanation for 21-cm absorption at cosmic dawn, Eur. Phys. J. C **78**, 746 (2018).
[28] A. Falkowski and K. Petraki, 21 cm absorption signal from charge sequestration, arXiv:1803.10096.
[29] G. Lambiase and S. Mohanty, Hydrogen spin oscillations in a background of axions and the 21-cm brightness temperature, Mon. Not. R. Astron. Soc. **494**, 5961 (2020).
[30] P. Sharma, Astrophysical radio background cannot explain the EDGES 21-cm signal: Constraints from cooling of non-thermal electrons, Mon. Not. R. Astron. Soc. **481**, L6 (2018).
[31] L.-B. Jia, Dark photon portal dark matter with the 21-cm anomaly, Eur. Phys. J. C **79**, 80 (2019).
[32] T. Moroi, K. Nakayama, and Y. Tang, Axion-photon conversion and effects on 21 cm observation, Phys. Lett. B **783**, 301 (2018).
[33] N. Houston, C. Li, T. Li, Q. Yang, and X. Zhang, Natural Explanation for 21 cm Absorption Signals via Axion-Induced Cooling, Phys. Rev. Lett. **121**, 111301 (2018).
[34] P. Sikivie, Axion dark matter and the 21-cm signal, Phys. Dark Universe **24**, 100289 (2019).
[35] A. Auriol, S. Davidson, and G. Raffelt, Axion absorption and the spin temperature of primordial hydrogen, Phys. Rev. D **99**, 023013 (2019).
[36] C. Li, N. Houston, T. Li, Q. Yang, and X. Zhang, A detailed exploration of the EDGES 21 cm absorption anomaly and axion-induced cooling, Int. J. Mod. Phys. D **30**, 2150041 (2021).
[37] M. Dhuria, Anomalous EDGES 21-cm signal and a moduli dominated era, Phys. Rev. D **100**, 103007 (2019).
[38] J. B. Muñoz, C. Dvorkin, and A. Loeb, 21-cm Fluctuations from Charged Dark Matter, Phys. Rev. Lett. **121**, 121301 (2018).
[39] J. R. Bhatt, A. K. Mishra, and A. C. Nayak, Viscous dark matter and 21 cm cosmology, Phys. Rev. D **100**, 063539 (2019).
[40] H. Liu, N. J. Outmezguine, D. Redigolo, and T. Volansky, Reviving millicharged dark matter for 21-cm cosmology, Phys. Rev. D **100**, 123011 (2019).
[41] K. Choi, H. Seong, and S. Yun, Axion-photon-dark photon oscillation and its implication for 21 cm observation, Phys. Rev. D **102**, 075024 (2020).
[42] P. K. Natwariya and J. R. Bhatt, EDGES signal in the presence of magnetic fields, Mon. Not. R. Astron. Soc. **497**, L35 (2020).
[43] L. Johns and S. Koren, The hydrogen mixing portal, its origins, and its cosmological effects, arXiv:2012.06591.
[44] A. Mathur, S. Rajendran, and H. Ramani, A composite solution to the EDGES anomaly, arXiv:2102.11284 [Phys. Rev. D (to be published)].
[45] F. Melia, The anomalous 21-cm absorption at high redshifts, Eur. Phys. J. C **81**, 230 (2021).

[46] M. Dhuria, V. Karambelkar, V. Rentala, and P. Sarmah, A strong broadband 21 cm cosmological signal from dark matter spin-flip interactions, J. Cosmol. Astropart. Phys. 08 (2021) 041.
[47] R. Thériault, J. T. Mirocha, and R. Brandenberger, Global 21 cm absorption signal from superconducting cosmic strings, J. Cosmol. Astropart. Phys. 10 (2021) 046.
[48] A. Aboubrahim, P. Nath, and Z.-Y. Wang, EDGES data as a signal of the Stueckelberg mechanism in the early universe, J. High Energy Phys. 12 (2021) 148.
[49] Q. Li and Z. Liu, Two-component millicharged dark matter and the EDGES 21 cm signal, Chin. Phys. C **46**, 045102 (2022).
[50] R. Hills, G. Kulkarni, P. D. Meerburg, and E. Puchwein, Concerns about modelling of the EDGES data, Nature (London) **564**, E32 (2018).
[51] J. D. Bowman, A. E. E. Rogers, R. A. Monsalve, T. J. Mozdzen, and N. Mahesh, Reply to Hills *et al.*, Nature (London) **564**, E35 (2018).
[52] R. F. Bradley, K. Tauscher, D. Rapetti, and J. O. Burns, A ground plane artifact that induces an absorption profile in averaged spectra from global 21-cm measurements—with possible application to EDGES, Astrophys. J. **874**, 153 (2019).
[53] K. Tauscher, D. Rapetti, and J. O. Burns, Formulating and critically examining the assumptions of global 21-cm signal analyses: How to avoid the false troughs that can appear in single spectrum fits, Astrophys. J. **897**, 132 (2020).
[54] S. Singh and R. Subrahmanyan, The redshifted 21-cm signal in the EDGES low-band spectrum, arXiv:1903.04540.
[55] S. Singh, T. J. Nambissan, R. Subrahmanyan, N. U. Shankar, B. S. Girish, A. Raghunathan *et al.*, On the detection of a cosmic dawn signal in the radio background, arXiv:2112.06778.
[56] A. M. Green, Dark matter in astrophysics/cosmology, SciPost Phys. Lect. Notes **37**, 1 (2022).
[57] L. E. Strigari, Galactic searches for dark matter, Phys. Rep. **531**, 1 (2013).
[58] A. Arbey and F. Mahmoudi, Dark matter and the early Universe: A review, Prog. Part. Nucl. Phys. **119**, 103865 (2021).
[59] S. S. Brems, B. M. Schäfer, N. Bucciantini, H. Keppler, M. Pössel, J. C. Strauß *et al.*, The dark universe—exercises and proceedings from the German-Italian WE heraeus summer school held in 2017 in Heidelberg, arXiv:1808.07551.
[60] M. Lisanti, Lectures on dark matter physics, in *Theoretical Advanced Study Institute in Elementary Particle Physics: New Frontiers in Fields and Strings* (2017), pp. 399–446, https://arxiv.org/pdf/1603.03797.pdf.
[61] G. Bertone and D. Hooper, History of dark matter, Rev. Mod. Phys. **90**, 045002 (2018).
[62] A. M. Green and B. J. Kavanagh, Primordial black holes as a dark matter candidate, J. Phys. G **48**, 043001 (2021).
[63] B. Carr and F. Kuhnel, Primordial black holes as dark matter candidates, in *Les Houches Summer School on Dark Matter* (2021), https://arxiv.org/pdf/2110.02821.pdf.
[64] B. Carr and F. Kuhnel, Primordial black holes as dark matter: Recent developments, Annu. Rev. Nucl. Part. Sci. **70**, 355 (2020).
[65] B. Carr, K. Kohri, Y. Sendouda, and J. Yokoyama, Constraints on primordial black holes, Rep. Prog. Phys. **84**, 116902 (2021).
[66] P. Villanueva-Domingo, O. Mena, and S. Palomares-Ruiz, A brief review on primordial black holes as dark matter, Front. Astron. Space Sci. **8**, 87 (2021).
[67] C. T. Byrnes and P. S. Cole, Lecture notes on inflation and primordial black holes, arXiv:2112.05716.
[68] N. Bhaumik and R. K. Jain, Primordial black holes dark matter from inflection point models of inflation and the effects of reheating, J. Cosmol. Astropart. Phys. 01 (2020) 037.
[69] R.-G. Cai, Z.-K. Guo, J. Liu, L. Liu, and X.-Y. Yang, Primordial black holes and gravitational waves from parametric amplification of curvature perturbations, J. Cosmol. Astropart. Phys. 06 (2020) 013.
[70] N. Bhaumik and R. K. Jain, Small scale induced gravitational waves from primordial black holes, a stringent lower mass bound, and the imprints of an early matter to radiation transition, Phys. Rev. D **104**, 023531 (2021).
[71] M. Y. Khlopov, Primordial black holes, Res. Astron. Astrophys. **10**, 495 (2010).
[72] K. M. Belotsky, V. I. Dokuchaev, Y. N. Eroshenko, E. A. Esipova, M. Y. Khlopov, L. A. Khromykh, A. A. Kirillov, V. V. Nikulin, S. G. Rubin, and I. V. Svadkovsky, Clusters of primordial black holes, Eur. Phys. J. C **79**, 246 (2019).
[73] S. V. Ketov and M. Y. Khlopov, Cosmological probes of supersymmetric field theory models at superhigh energy scales, Symmetry **11**, 511 (2019).
[74] S. W. Hawking, Particle creation by black holes, Commun. Math. Phys. **43**, 199 (1975).
[75] V. De Luca, G. Franciolini, P. Pani, and A. Riotto, Constraints on primordial black holes: The importance of accretion, Phys. Rev. D **102**, 043505 (2020).
[76] D. N. Page, Particle emission rates from a black hole: Massless particles from an uncharged, nonrotating hole, Phys. Rev. D **13**, 198 (1976).
[77] A. Arbey, J. Auffinger, and J. Silk, Evolution of primordial black hole spin due to Hawking radiation, Mon. Not. R. Astron. Soc. **494**, 1257 (2020).
[78] R. Laha, J. B. Muñoz, and T. R. Slatyer, INTEGRAL constraints on primordial black holes and particle dark matter, Phys. Rev. D **101**, 123514 (2020).
[79] J. H. MacGibbon and B. J. Carr, Cosmic rays from primordial black holes, Astrophys. J. **371**, 447 (1991).
[80] V. Poulin, J. Lesgourgues, and P. D. Serpico, Cosmological constraints on exotic injection of electromagnetic energy, J. Cosmol. Astropart. Phys. 03 (2017) 043.
[81] R. Laha, Primordial Black Holes as a Dark Matter Candidate Are Severely Constrained by the Galactic Center 511 keV γ-Ray Line, Phys. Rev. Lett. **123**, 251101 (2019).
[82] M. Boudaud and M. Cirelli, Voyager 1 $e^{\pm}$ Further Constrain Primordial Black Holes as Dark Matter, Phys. Rev. Lett. **122**, 041104 (2019).
[83] A. Coogan, L. Morrison, and S. Profumo, Direct Detection of Hawking Radiation from Asteroid-Mass Primordial Black Holes, Phys. Rev. Lett. **126**, 171101 (2021).

[84] B. Dasgupta, R. Laha, and A. Ray, Neutrino and Positron Constraints on Spinning Primordial Black Hole Dark Matter, Phys. Rev. Lett. **125**, 101101 (2020).
[85] A. Arbey, J. Auffinger, and J. Silk, Constraining primordial black hole masses with the isotropic gamma ray background, Phys. Rev. D **101**, 023010 (2020).
[86] R. Laha, P. Lu, and V. Takhistov, Gas heating from spinning and non-spinning evaporating primordial black holes, Phys. Lett. B **820**, 136459 (2021).
[87] S. J. Clark, B. Dutta, Y. Gao, L. E. Strigari, and S. Watson, Planck constraint on relic primordial black holes, Phys. Rev. D **95**, 083006 (2017).
[88] C. M. Lee and M. Ho Chan, The evaporating primordial black hole fraction in cool-core galaxy clusters, Astrophys. J. **912**, 24 (2021).
[89] M. H. Chan and C. M. Lee, Constraining primordial black hole fraction at the galactic centre using radio observational data, Mon. Not. R. Astron. Soc. **497**, 1212 (2020).
[90] V. Poulin, J. Lesgourgues, and P. D. Serpico, Cosmological constraints on exotic injection of electromagnetic energy, J. Cosmol. Astropart. Phys. 03 (2017) 043.
[91] T. Siegert, C. Boehm, F. Calore, R. Diehl, M. G. H. Krause, P. D. Serpico, and A. C. Vincent, Reticulum II: Particle dark matter and primordial black holes limits, Mon. Not. R. Astron. Soc. **511**, 914 (2022).
[92] J. Iguaz, P. D. Serpico, and T. Siegert, Isotropic X-ray bound on primordial black hole dark matter, Phys. Rev. D **103**, 103025 (2021).
[93] C. Keith and D. Hooper, 511 keV excess and primordial black holes, Phys. Rev. D **104**, 063033 (2021).
[94] G. Domènech, V. Takhistov, and M. Sasaki, Exploring evaporating primordial black holes with gravitational waves, Phys. Lett. B **823**, 136722 (2021).
[95] F. Schiavone, D. Montanino, A. Mirizzi, and F. Capozzi, Axion-like particles from primordial black holes shining through the Universe, J. Cosmol. Astropart. Phys. 08 (2021) 063.
[96] R.-G. Cai, Y.-C. Ding, X.-Y. Yang, and Y.-F. Zhou, Constraints on a mixed model of dark matter particles and primordial black holes from the galactic 511 keV line, J. Cosmol. Astropart. Phys. 03 (2021) 057.
[97] K. M. Belotsky, A. D. Dmitriev, E. A. Esipova, V. A. Gani, A. V. Grobov, M. Y. Khlopov, A. A. Kirillov, S. G. Rubin, and I. V. Svadkovsky, Signatures of primordial black hole dark matter, Mod. Phys. Lett. A **29**, 1440005 (2014).
[98] G. Ballesteros, J. Coronado-Blázquez, and D. Gaggero, X-ray and gamma-ray limits on the primordial black hole abundance from Hawking radiation, Phys. Lett. B **808**, 135624 (2020).
[99] S. Clark, B. Dutta, Y. Gao, Y.-Z. Ma, and L. E. Strigari, 21 cm limits on decaying dark matter and primordial black holes, Phys. Rev. D **98**, 043006 (2018).
[100] A. Halder, M. Pandey, D. Majumdar, and R. Basu, Exploring multimessenger signals from heavy dark matter decay with EDGES 21-cm result and IceCube, J. Cosmol. Astropart. Phys. 10 (2021) 033.
[101] A. Halder and S. Banerjee, Bounds on abundance of primordial black hole and dark matter from EDGES 21-cm signal, Phys. Rev. D **103**, 063044 (2021).
[102] A. Halder and M. Pandey, Investigating the effect of PBH, dark matter—baryon and dark matter—dark energy interaction on EDGES in 21 cm signal, Mon. Not. R. Astron. Soc. **508**, 3446 (2021).
[103] Y. Yang, Constraints on primordial black holes and curvature perturbations from the global 21-cm signal, Phys. Rev. D **102**, 083538 (2020).
[104] Y. Yang, The abundance of primordial black holes from the global 21 cm signal and extragalactic gamma-ray background, Eur. Phys. J. Plus **135**, 690 (2020).
[105] S. Mittal, A. Ray, G. Kulkarni, and B. Dasgupta, Constraining primordial black holes as dark matter using the global 21-cm signal with X-ray heating and excess radio background, J. Cosmol. Astropart. Phys. 03 (2022) 030.
[106] P. K. Natwariya, A. C. Nayak, and T. Srivastava, Constraining spinning primordial black holes with global 21 cm signal, Mon. Not. R. Astron. Soc. **510**, 4236 (2022).
[107] J. Cang, Y. Gao, and Y.-Z. Ma, 21-cm constraints on spinning primordial black holes, J. Cosmol. Astropart. Phys. 03 (2022) 012.
[108] M. Zaldarriaga, S. R. Furlanetto, and L. Hernquist, 21 centimeter fluctuations from cosmic gas at high redshifts, Astrophys. J. **608**, 622 (2004).
[109] S. A. Wouthuysen, On the excitation mechanism of the 21 cm interstellar hydrogen emission line, Physica (Utrecht) **18**, 75 (1952).
[110] G. B. Field, Excitation of the hydrogen 21-CM line, Proc. IRE **46**, 240 (1958).
[111] S. Furlanetto, S. P. Oh, and F. Briggs, Cosmology at low frequencies: The 21 cm transition and the high-redshift universe, Phys. Rep. **433**, 181 (2006).
[112] S. Mittal and G. Kulkarni, Ly α coupling and heating at cosmic dawn, Mon. Not. R. Astron. Soc. **503**, 4264 (2021).
[113] P. J. E. Peebles, Recombination of the primeval plasma, Astrophys. J. **153**, 1 (1968).
[114] Y. B. Zel'dovich, V. G. Kurt, and R. A. Syunyaev, Recombination of hydrogen in the hot model of the universe, Sov. J. Exp. Theor. Phys. **28**, 146 (1969), https://ui.adsabs.harvard.edu/abs/1969JETP...28..146Z/abstract.
[115] D. N. Page, Particle emission rates from a black hole. 2. Massless particles from a rotating hole, Phys. Rev. D **14**, 3260 (1976).
[116] J. H. MacGibbon and B. R. Webber, Quark and gluon jet emission from primordial black holes: The instantaneous spectra, Phys. Rev. D **41**, 3052 (1990).
[117] A. Arbey and J. Auffinger, BlackHawk: A public code for calculating the Hawking evaporation spectra of any black hole distribution, Eur. Phys. J. C **79**, 693 (2019).
[118] A. Arbey and J. Auffinger, Physics beyond the standard model with BlackHawk v2.0, Eur. Phys. J. C **81**, 910 (2021).
[119] H. Liu, T. R. Slatyer, and J. Zavala, Contributions to cosmic reionization from dark matter annihilation and decay, Phys. Rev. D **94**, 063507 (2016).
[120] T. R. Slatyer and C.-L. Wu, General constraints on dark matter decay from the cosmic microwave background, Phys. Rev. D **95**, 023010 (2017).
[121] T. R. Slatyer, Indirect dark matter signatures in the cosmic dark ages II. Ionization, heating and photon production

from arbitrary energy injections, Phys. Rev. D **93**, 023521 (2016).
[122] H. Liu, G. W. Ridgway, and T. R. Slatyer, Code package for calculating modified cosmic ionization and thermal histories with dark matter and other exotic energy injections, Phys. Rev. D **101**, 023530 (2020).
[123] A. Caputo, H. Liu, S. Mishra-Sharma, M. Pospelov, J. T. Ruderman, and A. Urbano, Edges and Endpoints in 21-cm Observations from Resonant Photon Production, Phys. Rev. Lett. **127**, 011102 (2021).
[124] D. J. Fixsen, A. Kogut, S. Levin, M. Limon, P. Lubin, P. Mirel *et al.*, ARCADE 2 Measurement of the Absolute Sky Brightness at 3–90 GHz, Astrophys. J. **734**, 5 (2011).
[125] J. Dowell and G. B. Taylor, The radio background below 100 MHz, Astrophys. J. Lett. **858**, L9 (2018).
[126] S. Chen, H.-H. Zhang, and G. Long, Revisiting the constraints on primordial black hole abundance with the isotropic gamma ray background, Phys. Rev. D **105**, 063008 (2022).
[127] H. Kim, A constraint on light primordial black holes from the interstellar medium temperature, Mon. Not. R. Astron. Soc. **504**, 5475 (2021).
[128] J. B. Muñoz, E. D. Kovetz, and Y. Ali-Haïmoud, Heating of baryons due to scattering with dark matter during the dark ages, Phys. Rev. D **92**, 083528 (2015).
[129] T. R. Slatyer and C.-L. Wu, Early-Universe constraints on dark matter-baryon scattering and their implications for a global 21 cm signal, Phys. Rev. D **98**, 023013 (2018).
[130] J. C. Hill and E. J. Baxter, Can early dark energy explain EDGES?, J. Cosmol. Astropart. Phys. 08 (2018) 037.
[131] S. Seager, D. D. Sasselov, and D. Scott, A new calculation of the recombination epoch, Astrophys. J. Lett. **523**, L1 (1999).
[132] S. Seager, D. D. Sasselov, and D. Scott, How exactly did the universe become neutral?, Astrophys. J. Suppl. Ser. **128**, 407 (2000).
[133] A. Fialkov, R. Barkana, A. Pinhas, and E. Visbal, Complete history of the observable 21-cm signal from the first stars during the pre-reionization era, Mon. Not. R. Astron. Soc. **437**, L36 (2014).
[134] A. Cohen, A. Fialkov, R. Barkana, and M. Lotem, Charting the parameter space of the global 21-cm signal, Mon. Not. R. Astron. Soc. **472**, 1915 (2017).
[135] R. Barkana, Possible interaction between baryons and dark-matter particles revealed by the first stars, Nature (London) **555**, 71 (2018).
[136] K. Cheung, J.-L. Kuo, K.-W. Ng, and Y.-L. S. Tsai, The impact of EDGES 21-cm data on dark matter interactions, Phys. Lett. B **789**, 137 (2019).
[137] M. Choudhury, A. Datta, and A. Chakraborty, Extracting the 21 cm Global signal using artificial neural networks, Mon. Not. R. Astron. Soc. **491**, 4031 (2020).
[138] J. O. Burns *et al.*, Dark cosmology: Investigating dark matter & exotic physics in the dark ages using the redshifted 21-cm global spectrum, arXiv:1902.06147.
[139] J. Burns, G. Hallinan, J. Lux, A. Romero-Wolf, L. Teitelbaum, T.-C. Chang *et al.*, FARSIDE: A low radio frequency interferometric array on the lunar farside, in *Bulletin of the American Astronomical Society* (2019), Vol. 51, p. 178, arXiv:1907.05407.
[140] A.-J. Boonstra, M. Garrett, G. Kruithof, M. Wise, A. van Ardenne, J. Yan *et al.*, Discovering the sky at the longest wavelengths (dsl), in *Proceedings of the 2016 IEEE Aerospace Conference* (2016), pp. 1–20, https://ieeexplore.ieee.org/document/7500678.
[141] A. Vecchio, M. Bentum, H. Falcke, A.-J. Boonstra, J. Ping, L. Chen *et al.*, The Netherlands-China low-frequency explorer (NCLE), in *Proceedings of the 43rd COSPAR Scientific Assembly. Held 28 January—4 February* (2021), Vol. 43, p. 1525, https://ui.adsabs.harvard.edu/abs/2021cosp...43E1525V/abstract.
[142] A. De Gouvêa, I. Martinez-Soler, Y. F. Perez-Gonzalez, and M. Sen, Fundamental physics with the diffuse supernova background neutrinos, Phys. Rev. D **102**, 123012 (2020).
[143] B. Dutta, A. Kar, and L. E. Strigari, Constraints on MeV dark matter and primordial black holes: Inverse Compton signals at the SKA, J. Cosmol. Astropart. Phys. 03 (2021) 011.
[144] S. Wang, D.-M. Xia, X. Zhang, S. Zhou, and Z. Chang, Constraining primordial black holes as dark matter at JUNO, Phys. Rev. D **103**, 043010 (2021).
[145] J. Cang, Y. Gao, and Y. Ma, Prospects of future CMB anisotropy probes for primordial black holes, J. Cosmol. Astropart. Phys. 05 (2021) 051.
[146] A. Ray, R. Laha, J. B. Muñoz, and R. Caputo, Near future MeV telescopes can discover asteroid-mass primordial black hole dark matter, Phys. Rev. D **104**, 023516 (2021).
[147] V. De Romeri, P. Martínez-Miravé, and M. Tórtola, Signatures of primordial black hole dark matter at DUNE and THEIA, J. Cosmol. Astropart. Phys. 10 (2021) 051.
[148] D. Ghosh, D. Sachdeva, and P. Singh, Future constraints on primordial black holes from XGIS-THESEUS, arXiv:2110.03333.
[149] A. Capanema, A. Esmaeili, and A. Esmaili, Evaporating primordial black holes in gamma ray and neutrino telescopes, J. Cosmol. Astropart. Phys. 12 (2021) 051.
[150] U. Mukhopadhyay, D. Majumdar, and A. Paul, Discriminating and constraining the synchrotron and inverse compton radiations from primordial black hole and dark matter at the galactic centre region, arXiv:2109.14955.